The role of the galaxy bispectrum and trispectrum for PNG detections in LSS

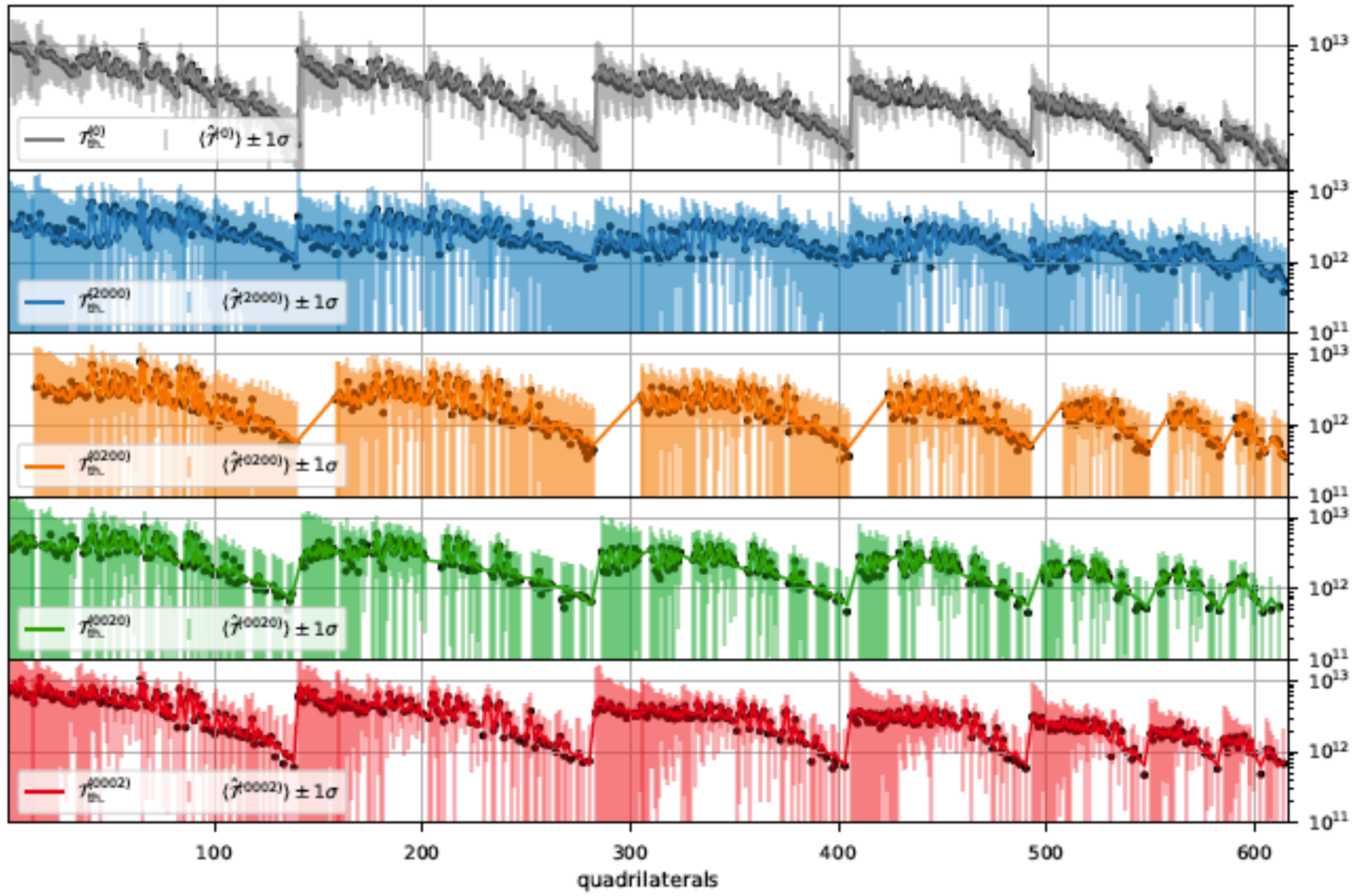

Héctor Gil-Marín, in collaboration with Davide Gualdi & Licia Verde
Institut de Ciències del Cosmos at U. Barcelona (ICCUB)

A window to fundamental physics, PNG and beyond. Madrid Sept. 2022

European Research Council

"la Caixa" Foundation

ICCUB Institut de Ciències del Cosmos UNIVERSITAT DE BARCELONA

Motivation

Scale dependent bias

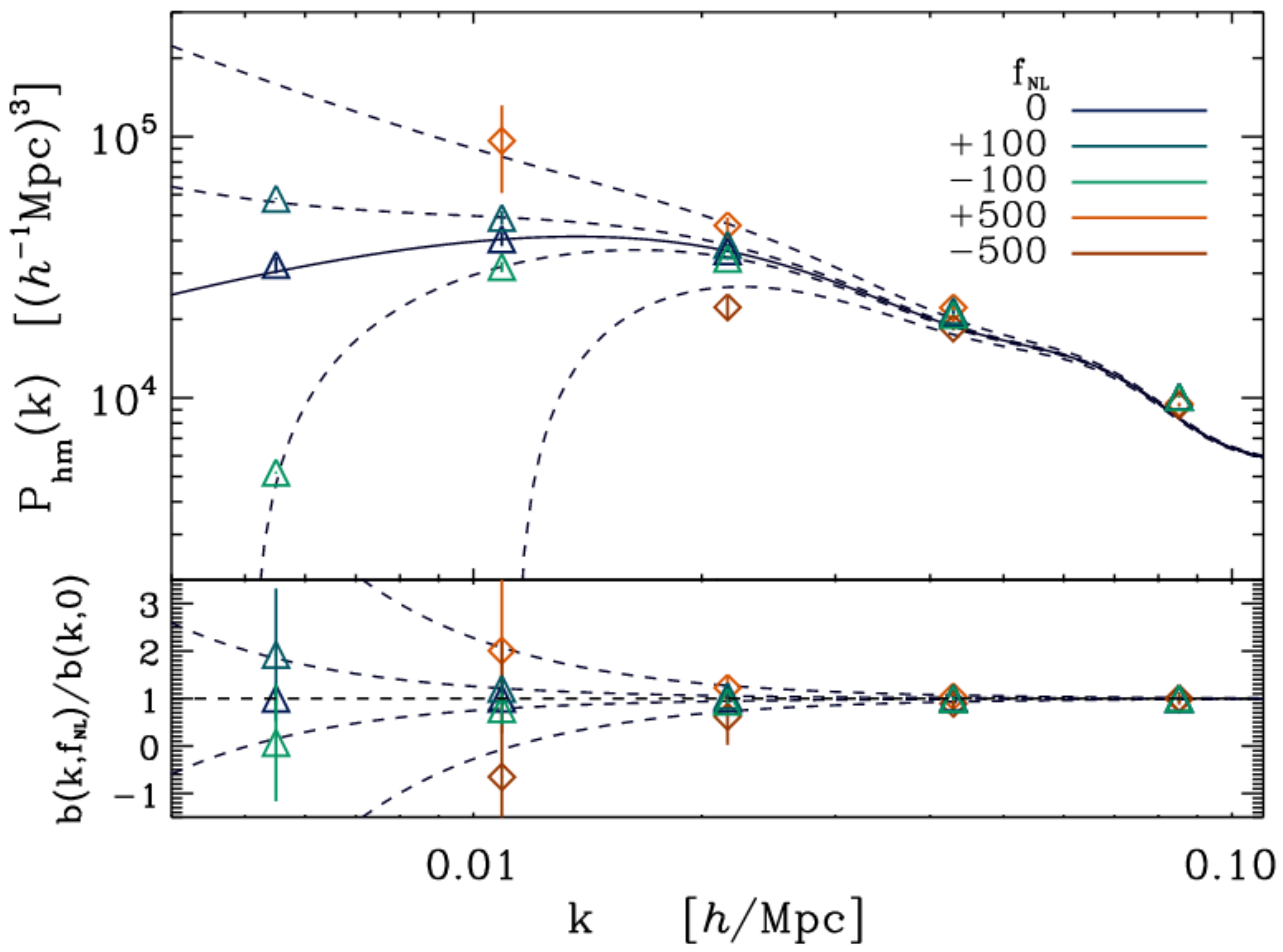

Dalal et al 2007. arXiv: 0710.4560

- Measuring f_{nl}, g_{nl} signal would be a direct probe of inflation.
- Current and on-going LSS data open a new window for this potential detection
- Main technique relies on the scale-dependent bias detection (see Eva's talk on eBOSS data).
- But it has drawbacks, we need to know very well galaxy formation and evolution (see Alex talk)
- **An alternative is a measurement of f_{nl} from the actual shape of the matter bispectrum and trispectrum**

Joint analysis of anisotropic power spectrum, bispectrum and trispectrum: application to N-body simulations

Davide Gualdi,[a,b] **Héctor Gil-Marín**[a,b] **and Licia Verde**[a,c]

[a]Institut de Ciències del Cosmos, University of Barcelona, ICCUB, Barcelona 08028, Spain
[b]Institute of Space Studies of Catalonia (IEEC), E-08034 Barcelona, Spain
[c]Institució Catalana de Recerca i Estudis Avançats, Passeig Lluís Companys 23, Barcelona 08010, Spain

E-mail: dgualdi@icc.ub.edu, hectorgil@icc.ub.edu, liciaverde@icc.ub.edu

JCAP Vol 2021, Issue 07, id.008

arXiv: 2104.03976

Summary Statistics

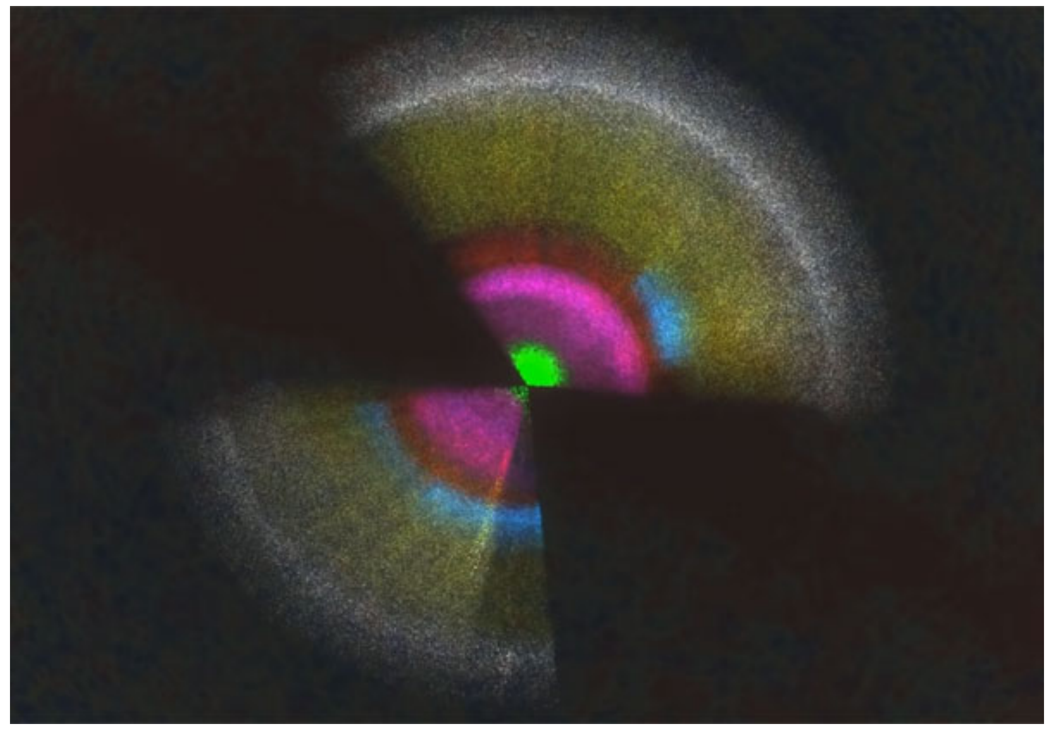

$$P(\mathbf{k}) \quad \oplus \quad B(\mathbf{k}_1, \mathbf{k}_2) \quad \oplus \quad T(\mathbf{k}_1, \mathbf{k}_2, \ldots)$$

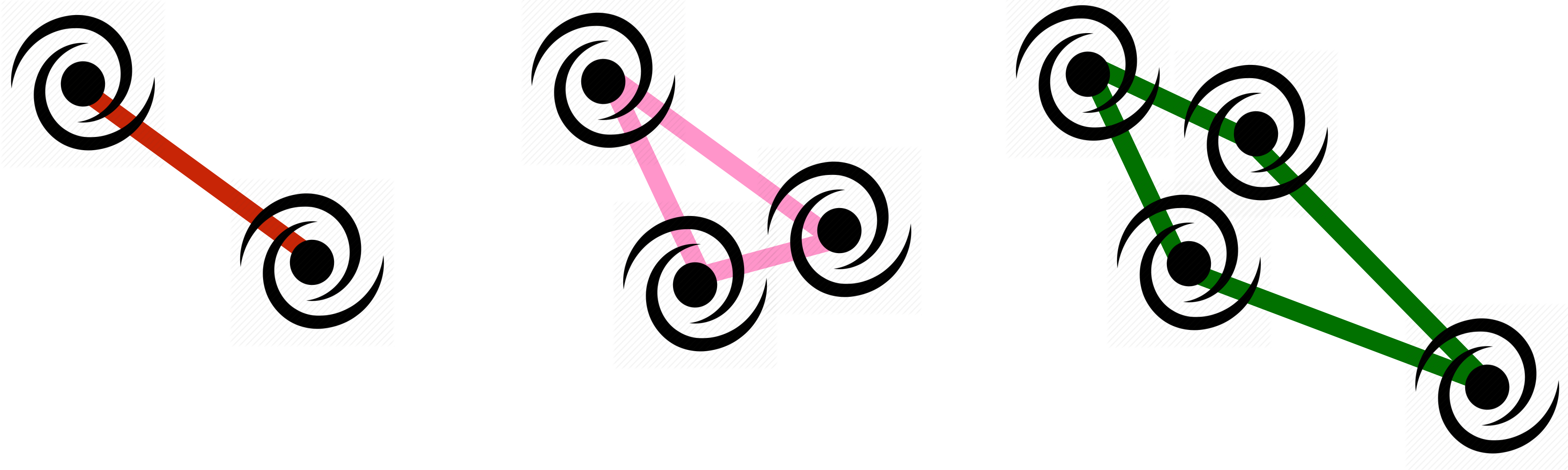

$$\langle \delta_k \delta_k' \rangle = P(\mathbf{k})\delta^D(\mathbf{k}+\mathbf{k}')$$
$$\langle \delta_{k_1}\delta_{k_2}\delta_{k_3} \rangle = B(\mathbf{k}_1,\mathbf{k}_2,\mathbf{k}_3)\delta^D(\mathbf{k}_1+\mathbf{k}_2+\mathbf{k}_3)$$
$$\langle \delta_{k_1}\delta_{k_2}\delta_{k_3}\delta_{k_4} \rangle = T(\mathbf{k}_1,\mathbf{k}_2,\mathbf{k}_3,\mathbf{k}_4)\delta^D(\mathbf{k}_1+\mathbf{k}_2+\mathbf{k}_3+\mathbf{k}_4)$$

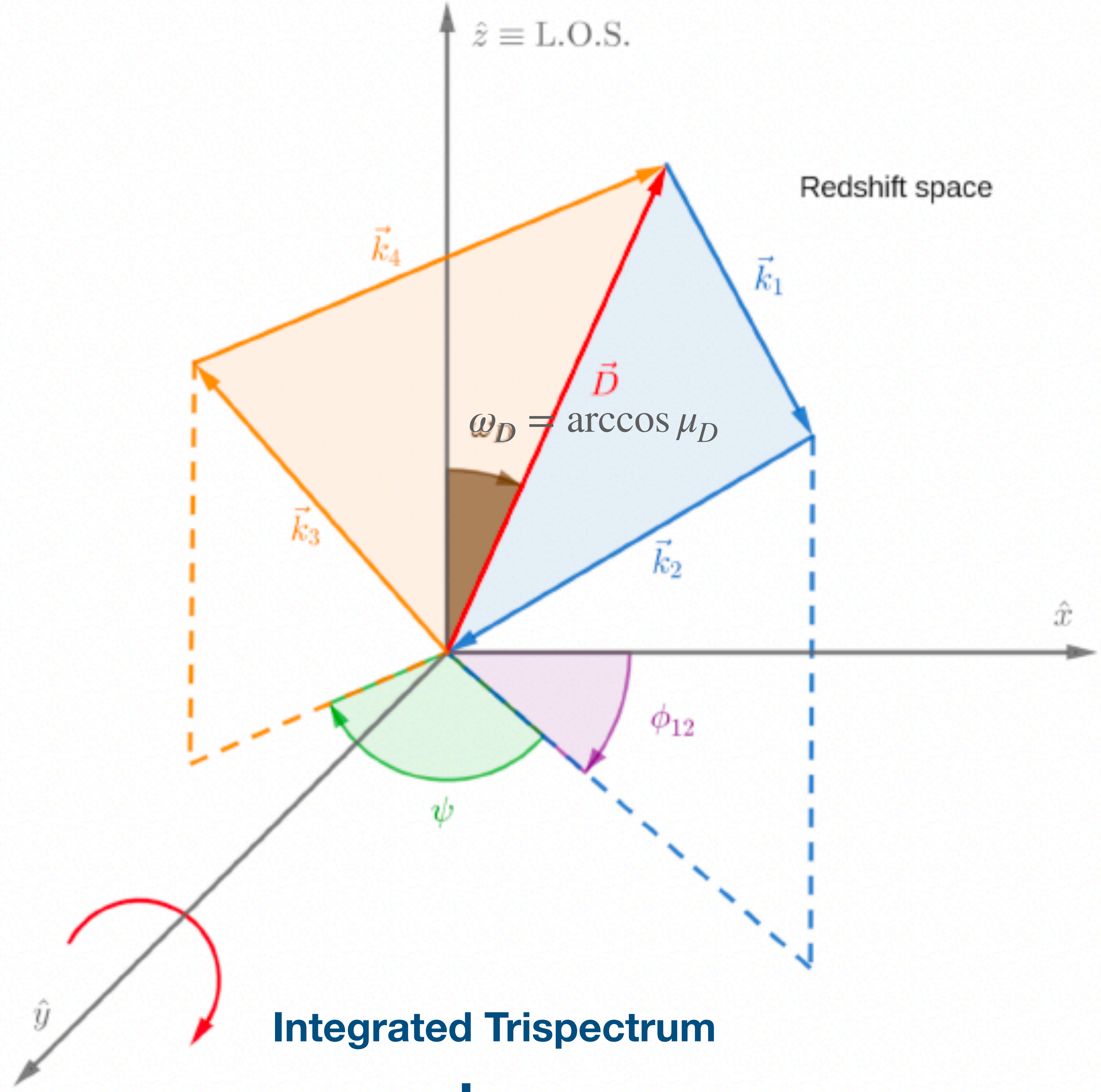

Line-of-sight expansion

Integrated Trispectrum

$$P^{(\ell)}(k) = \frac{(2\ell+1)}{2\alpha_\parallel \alpha_\perp^2} \int_{-1}^{+1} d\mu\, \mathcal{L}_\ell(\mu)\, P(p,\eta)$$

$$T^{(\ell_i)}(k_1,k_2,k_3,k_4) = \frac{1}{3} \sum_{\substack{k_1,k_2,k_3,k_4 \\ k_1,k_3,k_2,k_4 \\ k_1,k_2,k_4,k_3}} \frac{2\ell+1}{16\pi^2 \Delta D \alpha_\parallel^3 \alpha_\perp^6} \int_{D_{\rm min}}^{D_{\rm max}} dD \int_{-1}^{+1} d\mu_D \int_0^{2\pi} d\phi_{12} \int_0^{2\pi} d\psi \times \mathcal{L}_\ell(\mu_i) T^{\rm s}(p_1,p_2,p_3,p_4,D,\eta_D,\phi_{12},\psi)\,.$$

$$B^{(\ell_i)}(k_1,k_2,k_3) = \frac{(2\ell+1)}{8\pi\alpha_\parallel^2\alpha_\perp^4} \int_{-1}^{+1} d\mu_1 \int_0^{2\pi} d\phi\, \mathcal{L}_\ell(\mu_i) B(p_1,p_2,p_3,\eta_1,\eta_2)\,,$$

$$B^{(\ell_1)} = B^{(\ell,0,0)}; \quad B^{(\ell_2)} = B^{(0,\ell,0)}; \quad B^{(\ell_3)} = B^{(0,0,\ell)}$$

$$T^{(\ell_1)} = T^{(\ell,0,0,0)}; \quad T^{(\ell_2)} = T^{(0,\ell,0,0)}; \quad \ldots$$

$$B^{(0,2)} \equiv B^{(0)} \oplus B^{(2_1)} \oplus B^{(2_2)} \oplus B^{(2_3)}$$

$$T^{(0,2)} \equiv T^{(0)} \oplus T^{(2_1)} \oplus T^{(2_2)} \oplus T^{(2_3)} \oplus T^{(2_4)}$$

Summary Statistics

- We aim to use the **full P+B+T multipoles** to jointly constrain {α_{para}, α_{perp}, f, σ_8, f_{nl}}

BAO dilation scales

$$\alpha_{\parallel} \equiv \frac{D_H/r_s}{[D_H/r_s]^{\rm fid}}$$

$$\alpha_{\perp} \equiv \frac{D_M/r_s}{[D_M/r_s]^{\rm fid}}$$

RSD parameter

$$f(z) = \Omega_m(z)^\gamma$$

Primordial features

$$\sigma_8^2 = \int dk\, P_{\rm lin}(k, z=0) W_{TH}(k \cdot R_8)$$

$$f_{\rm nl}$$

- We use **Quijote** N-body sim 1 $[\mathrm{Gpc}/h]^3$ boxes to get the **data-vector** and its **covariance**
- We will run both Fisher-like and a Monte Carlo Markov Chain like analyses.
- The aim is to extract f_{nl} from the shape of the summary statistics.
- We will not employ the scale-dependent bias feature to measure f_{nl}

Summary Statistics

Theoretical modelling: Gravitational evolution

We take the SPT functional form for the tree-level expressions for both B and T

$$\begin{aligned} B_{\rm FPT}(\mathbf{k}_1,\mathbf{k}_2,\mathbf{k}_3) =& \ 2Z^{(1)}_{\rm FPT}[\mathbf{k}_1]\,Z^{(1)}_{\rm FPT}[\mathbf{k}_2]\,Z^{(2)}_{\rm FPT}[\mathbf{k}_1,\mathbf{k}_2]\ P(k_1)\,P(k_2) \\ +& \quad 2 \text{ permutations}\,, \end{aligned}$$

$$\begin{aligned} T_{\rm FPT}(\mathbf{k}_1,\mathbf{k}_2,\mathbf{k}_3,\mathbf{k}_4) =& \ 4P(k_1)P(k_2)Z^{(1)}_{\rm SPT}[\mathbf{k}_1]\,Z^{(1)}_{\rm SPT}[\mathbf{k}_2] \\ & \times \Big\{ Z^{(2)}_{\rm FPT}[\mathbf{k}_1,-\mathbf{k}_{13}]\,Z^{(2)}_{\rm FPT}[\mathbf{k}_2,\mathbf{k}_{13}]\,P(k_{13}) \\ & + Z^{(2)}_{\rm FPT}[\mathbf{k}_1,-\mathbf{k}_{14}]\,Z^{(2)}_{\rm FPT}[\mathbf{k}_2,\mathbf{k}_{14}]\,P(k_{14})\Big\} + 5\,\text{p.} \\ & + 6\ Z^{(1)}_{\rm SPT}[\mathbf{k}_1]\,Z^{(1)}_{\rm SPT}[\mathbf{k}_2]\,Z^{(1)}_{\rm SPT}[\mathbf{k}_3]\,Z^{(3)}_{\rm FPT}[\mathbf{k}_1,\mathbf{k}_2,\mathbf{k}_3]\,P(k_1)P(k_2)P(k_3) \\ & + \ 3\,\text{p.}, \end{aligned}$$

Promote the SPT kernels to an effective kernels (FPT) where we fit for f_1,f_2,f_3,g_1,g_2,g_3 (Scoccimarro 2001, Gil-Marin 2011,2014)

$$\begin{aligned} F^{(2)}_{\rm FPT}[\mathbf{k}_a,\mathbf{k}_b] &= f_1\,\frac{5}{7} + f_2\,\frac{1}{2}\frac{\mathbf{k}_a\cdot\mathbf{k}_b}{k_a k_b}\left(\frac{k_a}{k_b}+\frac{k_b}{k_a}\right) + f_3\,\frac{2}{7}\frac{(\mathbf{k}_a\cdot\mathbf{k}_b)^2}{k_a^2 k_b^2} \\ G^{(2)}_{\rm FPT}[\mathbf{k}_a,\mathbf{k}_b] &= g_1\,\frac{3}{7} + g_2\,\frac{1}{2}\frac{\mathbf{k}_a\cdot\mathbf{k}_b}{k_a k_b}\left(\frac{k_a}{k_b}+\frac{k_b}{k_a}\right) + g_3\,\frac{4}{7}\frac{(\mathbf{k}_a\cdot\mathbf{k}_b)^2}{k_a^2 k_b^2}\,. \end{aligned}$$

- Extend the k-range of validity of SPT
- Same f_i, g_i for different redshifts and cosmologies

Summary Statistics

Theoretical modelling: PNG (f_{nl})

$$B^{\rm PNG}(\mathbf{k}_1,\mathbf{k}_2,\mathbf{k}_3) = Z^{(1)}(k_1)Z^{(1)}(k_2)Z^{(1)}(k_3)\frac{\mathcal{M}(k_1)}{\mathcal{M}(k_2)\mathcal{M}(k_3)}\frac{2f_{\rm nl}}{c^2}P(k_2)P(k_3) \;+\; \text{cyc.}.$$

$$\begin{aligned} T^{\rm PNG}(\mathbf{k}_1,\mathbf{k}_2,\mathbf{k}_3,\mathbf{k}_4) = & \frac{f_{\rm nl}}{c^2}Z^{(1)}(k_1)Z^{(1)}(k_2)Z^{(1)}(k_3) \\ & \times \left\{ \left[4\frac{\mathcal{M}(k_1)}{\mathcal{M}(k_2)}P(k_2)P(k_3)\frac{P(|\mathbf{k}_3+\mathbf{k}_4|)}{\mathcal{M}(|\mathbf{k}_3+\mathbf{k}_4|)}Z^{(2)}_{\rm FPT}\left[-\mathbf{k}_3,\mathbf{k}_3+\mathbf{k}_4\right] \;+\; 5\,\text{p.}\right] \right. \\ & \left. + \left[2\frac{\mathcal{M}(|\mathbf{k}_3+\mathbf{k}_4|)}{\mathcal{M}(k_1)\mathcal{M}(k_2)}P(k_1)P(k_2)P(k_3)Z^{(2)}_{\rm FPT}\left[\mathbf{k}_3+\mathbf{k}_4,-\mathbf{k}_3\right] \;+\; 2\,\text{p.}\right] \right\} \\ & + 3\,\text{p.}. \end{aligned}$$

$$\mathscr{M}_k \equiv \frac{3}{5}k^2\mathbb{T}_k D_+/(\Omega_m H_0^2)$$

$\mathbb{T}_k$ Power Spectrum transfer function

Summary Statistics

Theoretical modelling: PNG (f_{nl})

$$B^{\rm PNG}(\mathbf{k}_1,\mathbf{k}_2,\mathbf{k}_3) = Z^{(1)}(k_1)Z^{(1)}(k_2)Z^{(1)}(k_3)\frac{\mathcal{M}(k_1)}{\mathcal{M}(k_2)\mathcal{M}(k_3)}\frac{2f_{\rm nl}}{c^2}P(k_2)P(k_3) + \text{cyc.}\,.$$

$$T^{\rm PNG}(\mathbf{k}_1,\mathbf{k}_2,\mathbf{k}_3,\mathbf{k}_4) = \frac{f_{\rm nl}}{c^2}Z^{(1)}(k_1)Z^{(1)}(k_2)Z^{(1)}(k_3) \times \left\{\left[4\frac{\mathcal{M}(k_1)}{\mathcal{M}(k_2)}P(k_2)P(k_3)\frac{P(|\mathbf{k}_3+\mathbf{k}_4|)}{\mathcal{M}(|\mathbf{k}_3+\mathbf{k}_4|)}Z^{(2)}_{\rm FPT}[-\mathbf{k}_3,\mathbf{k}_3+\mathbf{k}_4] + 5\,\text{p.}\right] + \left[2\frac{\mathcal{M}(|\mathbf{k}_3+\mathbf{k}_4|)}{\mathcal{M}(k_1)\mathcal{M}(k_2)}P(k_1)P(k_2)P(k_3)Z^{(2)}_{\rm FPT}[\mathbf{k}_3+\mathbf{k}_4,-\mathbf{k}_3] + 2\,\text{p.}\right]\right\} + 3\,\text{p.}\,.$$

In the bispectrum fnl signal is purely primordial, in the trispectrum it couples with $Z^{(2)}$ kernel (gravity)

$$\mathscr{M}_k \equiv \frac{3}{5}k^2\mathbb{T}_k D_+/(\Omega_m H_0^2)$$

$\mathbb{T}_k$ Power Spectrum transfer function

Methodology

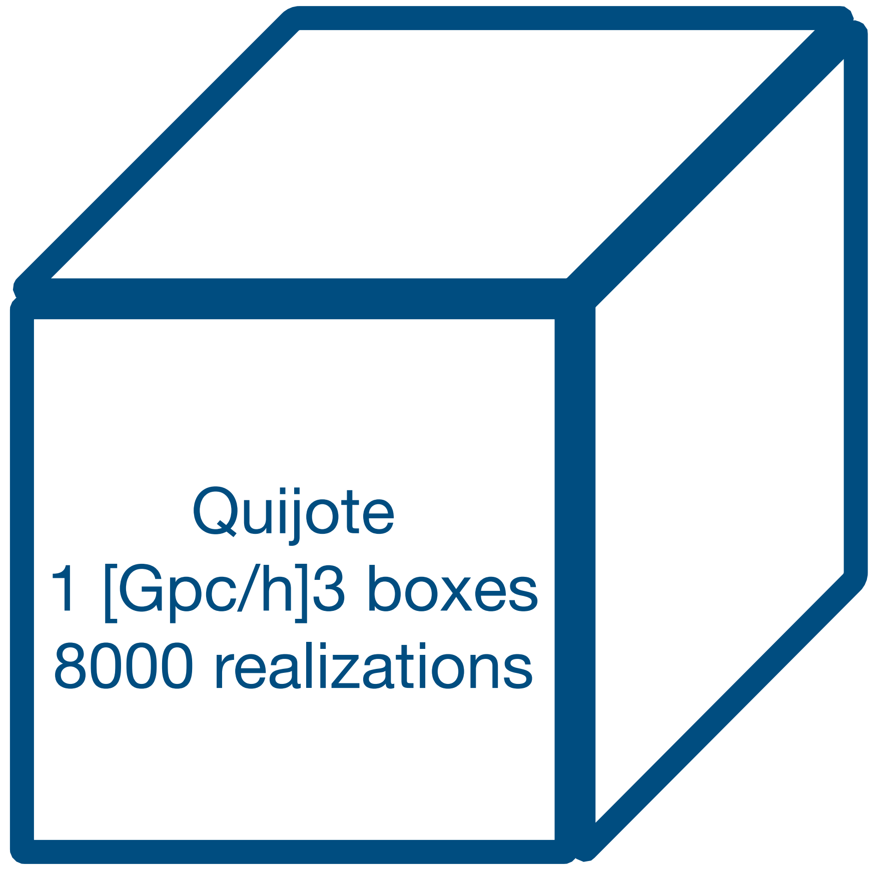

Dark Matter particles
Main density
downsample to match
galaxy density

$\bar{n} = 5 \cdot 10^{-4} [\mathrm{Mpc/h}]^{-3}$

3615 elements

$P^{(0,2)}$

$B^{(0,2)}$

$T^{(0,2)}$

$0.04 < k < 0.13 \quad P^{(0)}$

$0.06 < k < 0.13 \quad P^{(2)}$

$0.04 < k < 0.12 \quad B^{(0,2)};\ T^{(0,2)}$

Full PBT covariance matrix
(trispectrum-only covariance shown)

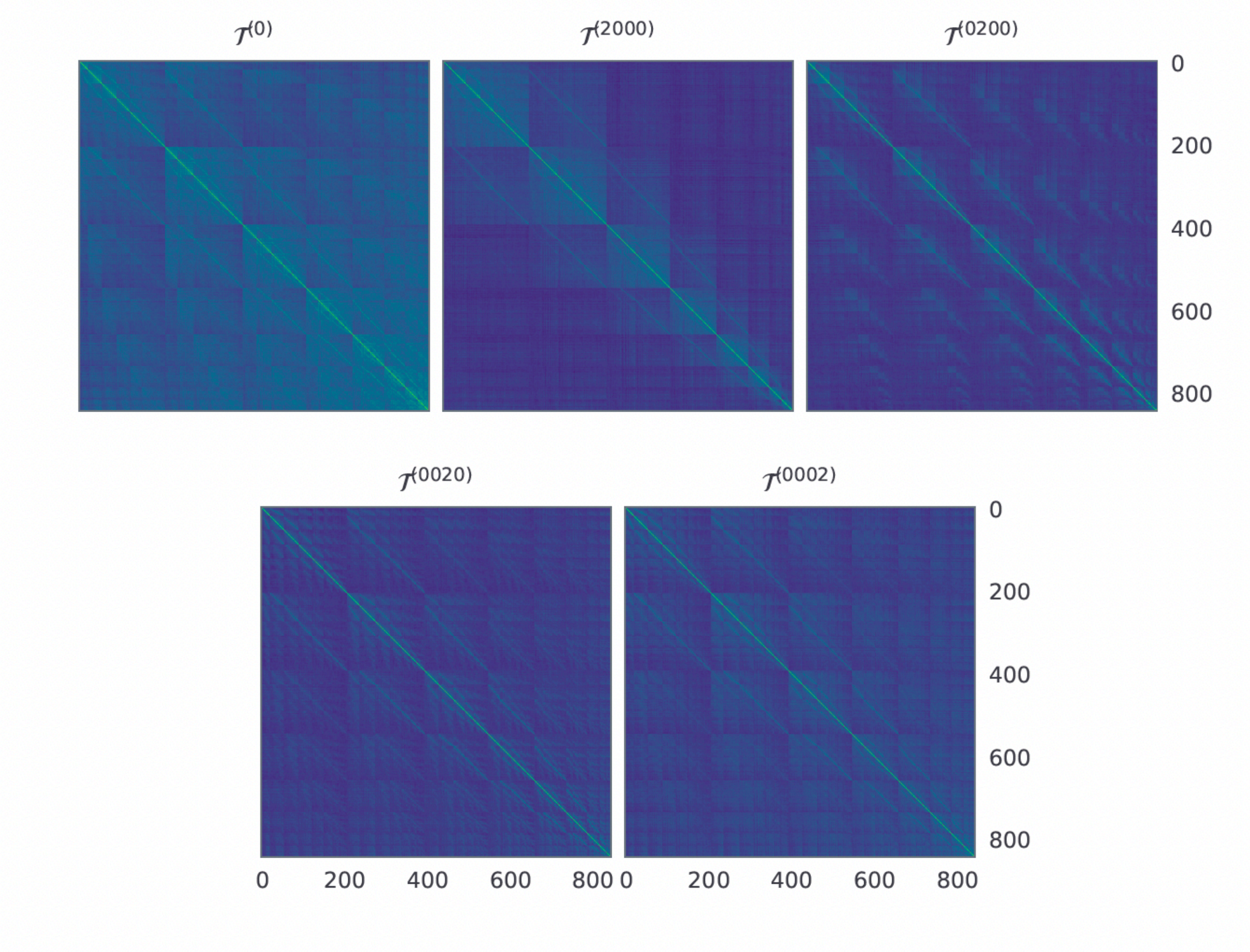

C_{ij}

Scaled to a volume of 25 [Gpc/h]^3

+ Sellentin & Heavens correction

DESI/LSST/ EUCLID like surveys

7 Nuisance / galaxy variables

Estimate the errors: 1) à la Fisher; 2) à la MCMC

$\{\alpha_{\parallel}, \alpha_{\perp}, f, \sigma_8, f_{\rm nl}, \mid b_1, b_2, b_3, A_{\rm noise}, \sigma_P, \sigma_B, \sigma_T\} \quad + b_{3\rm nl}, b_{s2}$

5 physical variables

2 non-local biases fixed to local Lagrangian

Simultaneously vary all of them, as if we were fitting an actual galaxy field

Results I. Signal-to-Noise

How much do we gain as we go to larger k-values?

$$\langle S/N \rangle = \frac{1}{N_{\rm sim}} \sum_{i=1}^{N_{\rm sim}} \sqrt{\hat{\mathbf{d}}_i^\intercal \, \mathbf{Cov}_{\mathbf{d}}^{-1} \, \hat{\mathbf{d}}_i} \,,$$

- Above k>0.1 adding higher order multipoles boosts SN.
- Adding bispectrum quadrupole is very complementary to trispectrum monopole

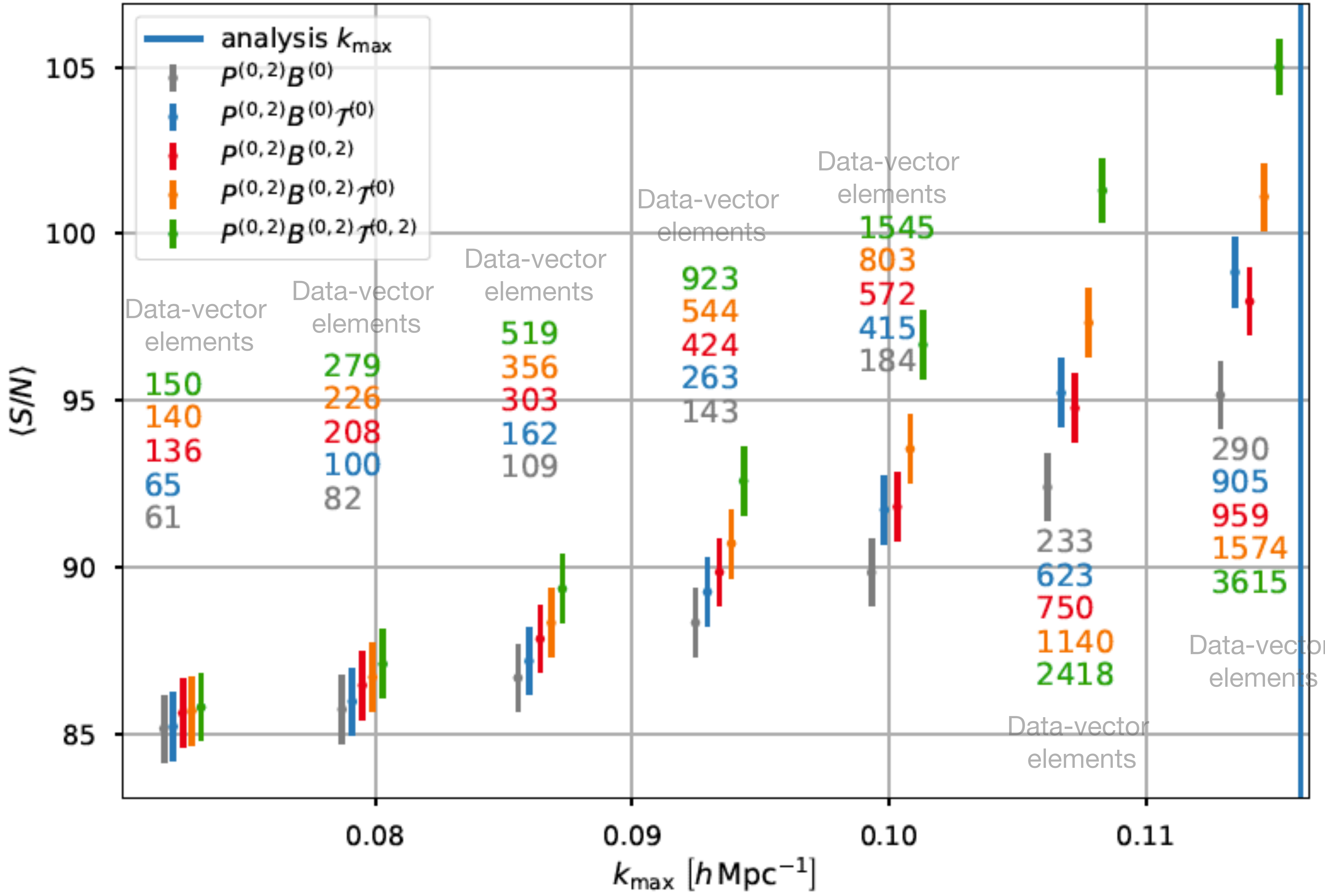

Results II. Fisher & MCMC

Fisher

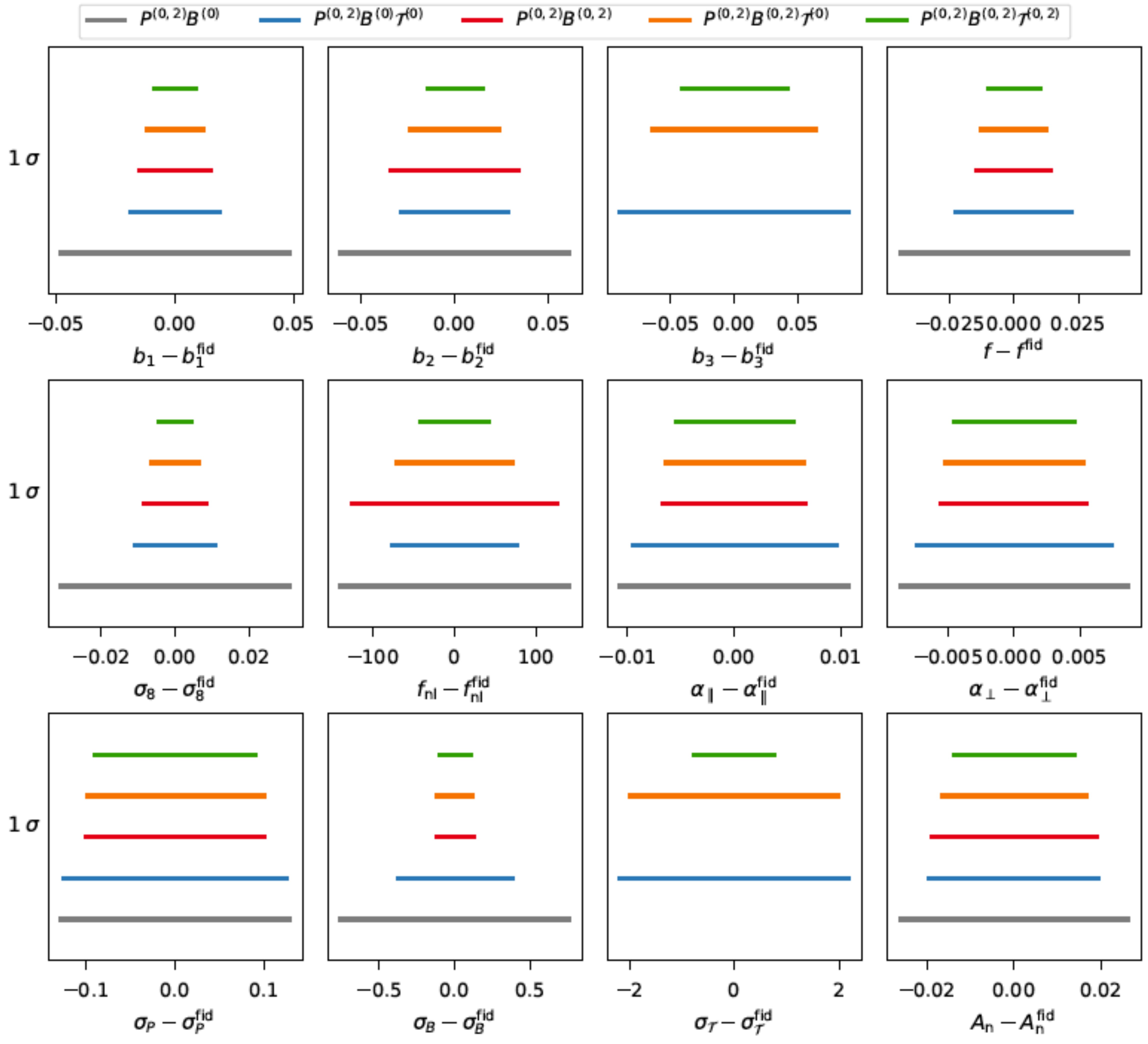

Monte Carlo Markov Chains

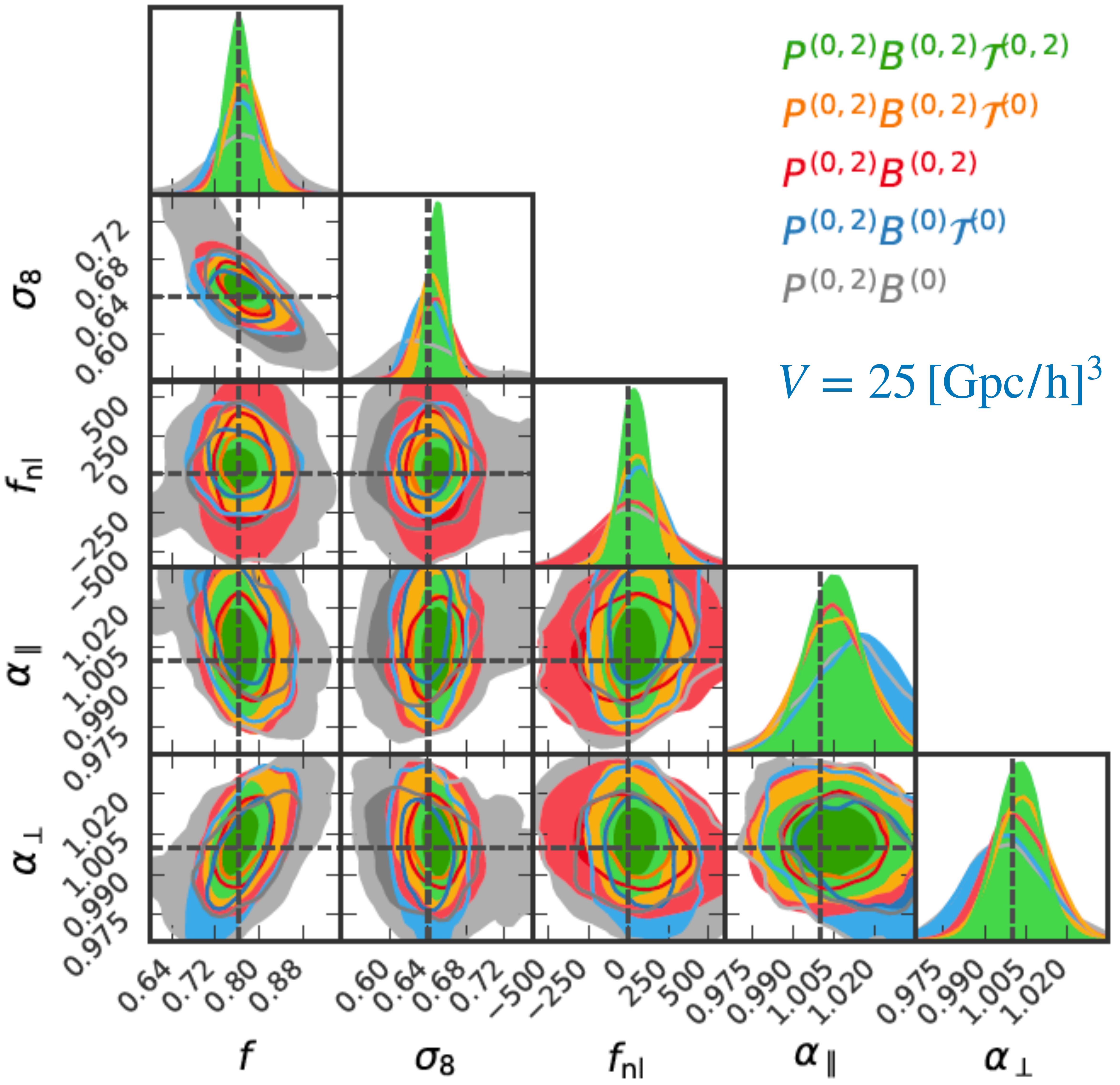

Results II. Fisher & MCMC

Fisher

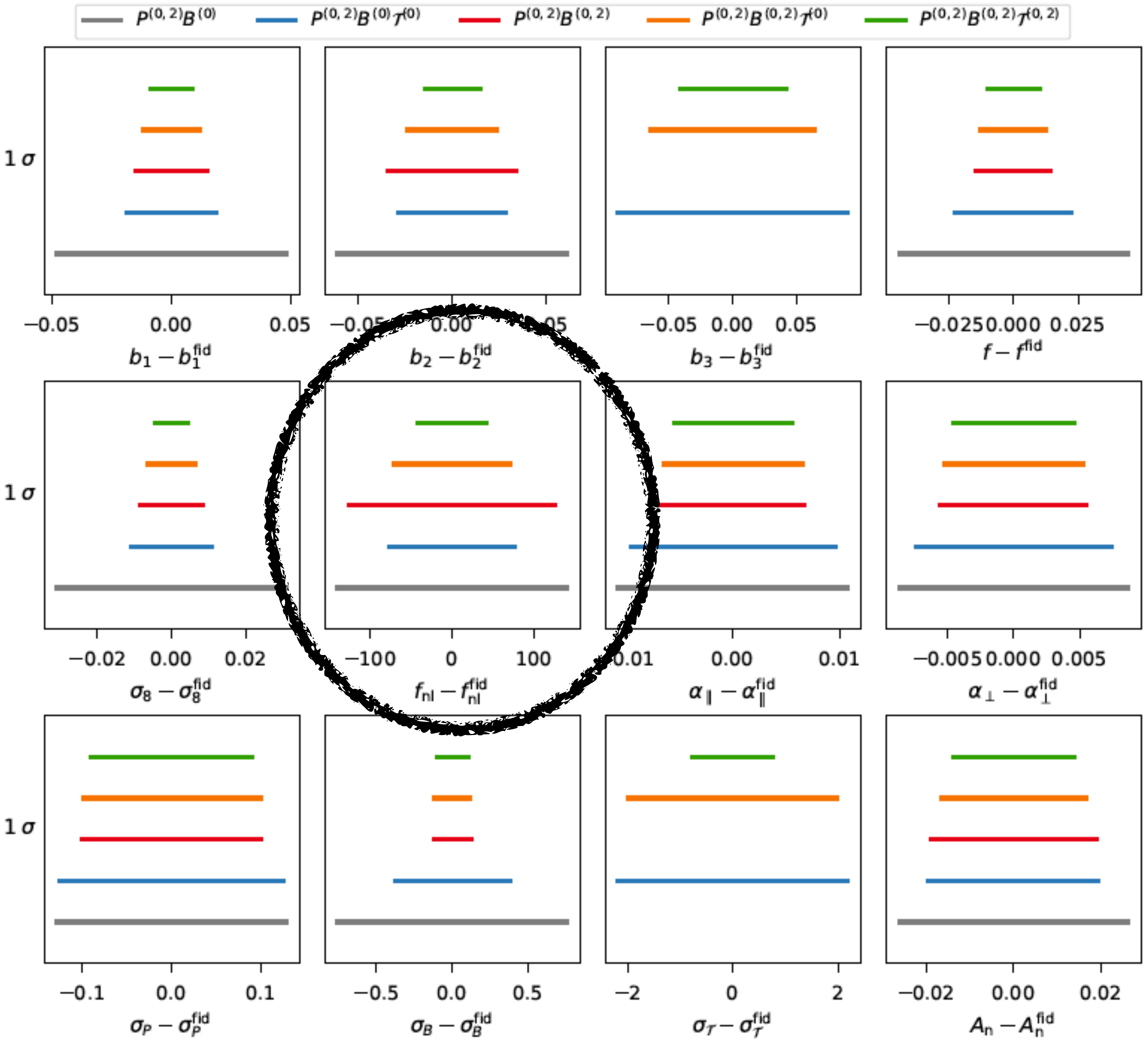

Monte Carlo Markov Chains

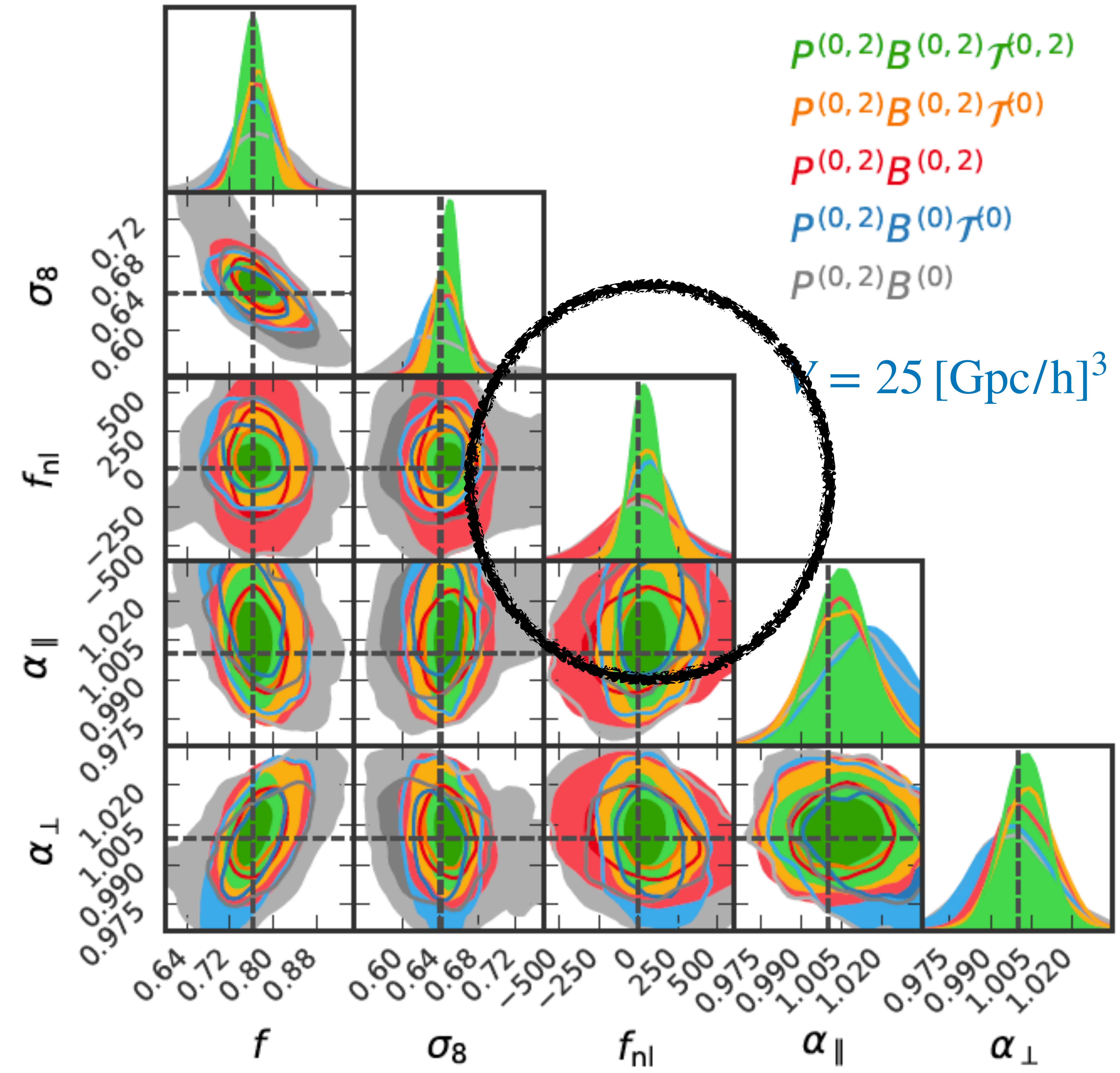

Results II. Fisher & MCMC

Parameter error
For $P_{(0,2)}$ $B^{(0)}$

MCMC (Fisher Forecasts) — $V = 25\,[\mathrm{Gpc/h}]^3$

	$\Delta\theta$	1 - $(\Delta\theta/\Delta\theta_{P^{(0,2)}B^{(0)}})$ [%]			
	$P^{(0,2)}B^{(0)}$	$P^{(0,2)}B^{(0)}\mathcal{T}^{(0)}$	$P^{(0,2)}B^{(0,2)}$	$P^{(0,2)}B^{(0,2)}\mathcal{T}^{(0)}$	$P^{(0,2)}B^{(0,2)}\mathcal{T}^{(0,2)}$
f	**0.140 (0.090)**	42.8 (48.8)	46.4 (66.8)	57.7 (70.4)	71.9 (76.5)
σ_8	**0.078 (0.062)**	52.3 (64.1)	40.6 (71.5)	62.3 (77.8)	78.2 (85.1)
$f_{\rm nl}$	**536 (282)**	49.1 (44.4)	9.5 (9.5)	55.1 (48.6)	71.7 (68.7)
$\alpha_{\parallel}$	**0.036 (0.022)**	13.9 (10.6)	30.6 (37.2)	34.2 (39)	46.8 (47.7)
$\alpha_{\perp}$	**0.032 (0.018)**	14.3 (14.5)	29.1 (35.8)	33 (39.2)	46.3 (46.3)
average improvement		31.3 (36.5)	32.1 (44.2)	44.6 (55)	61 (64.9)

$f_{\rm nl} = \pm\, 150$

Results II. Fisher & MCMC

Parameter error For $P_{(0,2)}$ $B^{(0)}$

	MCMC (Fisher Forecasts) $V = 25\,[\mathrm{Gpc/h}]^3$				
	$\Delta\theta$	1 - $(\Delta\theta/\Delta\theta_{P^{(0,2)}B^{(0)}})$ [%]			
	$P^{(0,2)}B^{(0)}$	$P^{(0,2)}B^{(0)}\mathcal{T}^{(0)}$	$P^{(0,2)}B^{(0,2)}$	$P^{(0,2)}B^{(0,2)}\mathcal{T}^{(0)}$	$P^{(0,2)}B^{(0,2)}\mathcal{T}^{(0,2)}$
f	**0.140 (0.090)**	42.8 (48.8)	46.4 (66.8)	57.7 (70.4)	71.9 (76.5)
σ_8	**0.078 (0.062)**	52.3 (64.1)	40.6 (71.5)	62.3 (77.8)	78.2 (85.1)
$f_{\rm nl}$	**536 (282)**	49.1 (44.4)	9.5 (9.5)	55.1 (48.6)	71.7 (68.7)
$\alpha_\parallel$	**0.036 (0.022)**	13.9 (10.6)	30.6 (37.2)	34.2 (39)	46.8 (47.7)
$\alpha_\perp$	**0.032 (0.018)**	14.3 (14.5)	29.1 (35.8)	33 (39.2)	46.3 (46.3)
average improvement		31.3 (36.5)	32.1 (44.2)	44.6 (55)	61 (64.9)

$f = \pm 0.040$

$\sigma_8 = \pm 0.017$

$f_{\rm nl} = \pm 150$

$\alpha_\parallel = \pm 0.019$

$\alpha_\perp = \pm 0.017$

Conclusions

- Covariance corresponds to 25 $[\mathrm{Gpc}/h]^3$ of order of what DESI/EUCLID/VR will map
- Number density of objects is similar to what you expect from LRGs 5×10^{-4}
- k-range for B & T is realistic to the current modelling techniques $0.04 < k < 0.12$
- We have marginalised over the rest of relevant cosmological variables, and bias parameters
- The covariance have been inferred from actual Nbody simulations
- **This approach is a complementary approach to the scale-dependent bias and does not rely on b_ϕ or p calibration issue. Complementarity => Robustness!**

$$f = \pm\, 0.040$$
$$\sigma_8 = \pm\, 0.017$$
$$f_{\rm nl} = \pm\, 150$$
$$\alpha_{\parallel} = \pm\, 0.019$$
$$\alpha_{\perp} = \pm\, 0.017$$

Results III. Trispectrum detection in BOSS

Detection of iT in BOSS DR12 LRG sample

Integrated trispectrum detection from BOSS DR12 NGC CMASS

Davide Gualdi,[a,b] and Licia Verde[a,c]

[a]Institut de Ciències del Cosmos, University of Barcelona, ICCUB, Barcelona 08028, Spain
[b]Institute of Space Studies of Catalonia (IEEC), E-08034 Barcelona, Spain
[c]Institució Catalana de Recerca i Estudis Avançats, Passeig Lluís Companys 23, Barcelona 08010, Spain

E-mail: dgualdi@icc.ub.edu, liciaverde@icc.ub.edu

2022arXiv220106932

- **Detection of iTrispectrum,**
- $T^{(0,0,0,0)}$ at 10.4σ
- $T^{(2,0,0,0)}$ at 5.2σ
- $T^{(0,2,0,0)}$ at 8.3σ
- $T^{(0,0,2,0)}$ at 1.1σ
- $T^{(0,0,0,2)}$ at 3.1σ

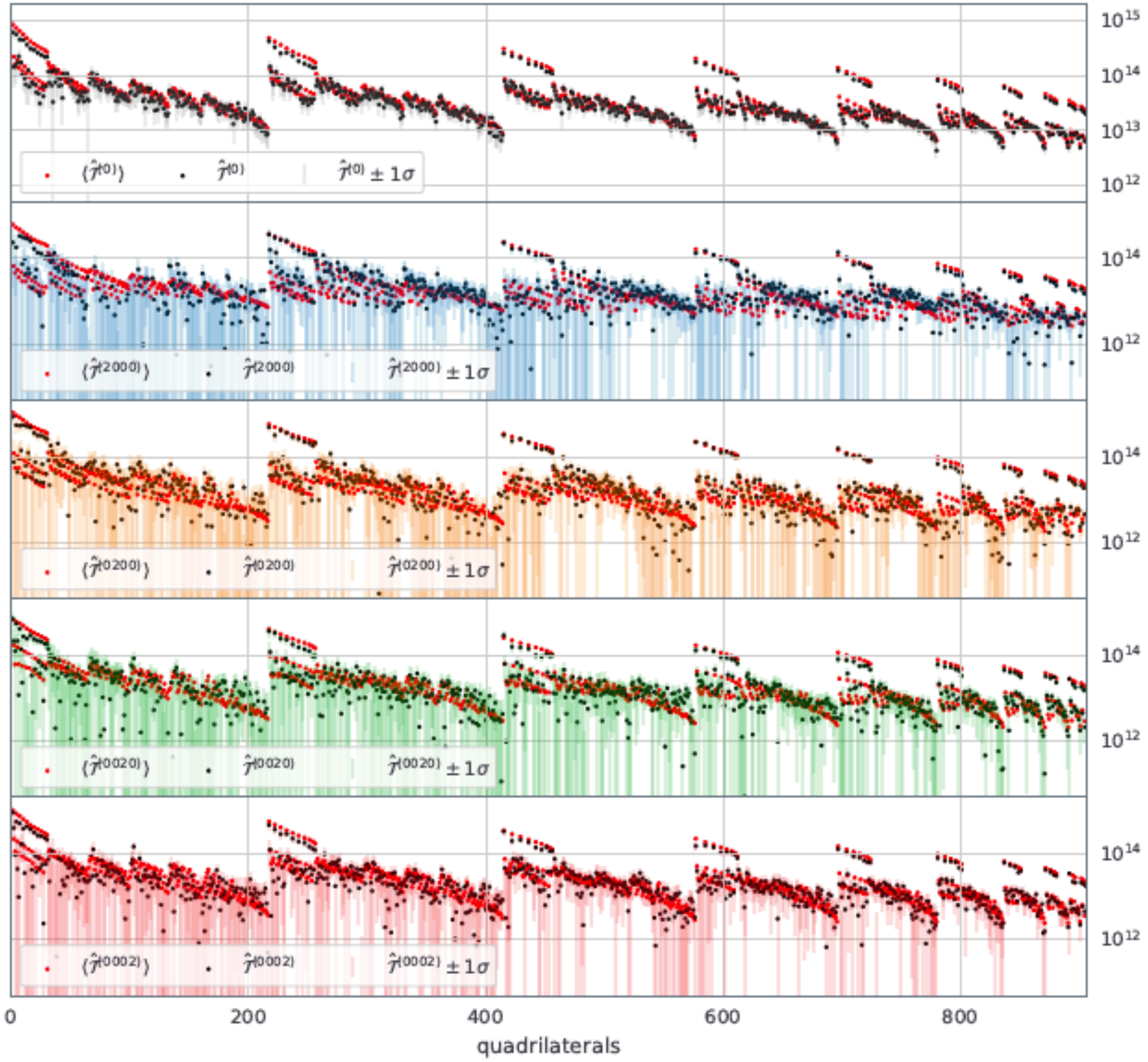

Bonus Slides

Full data-vector

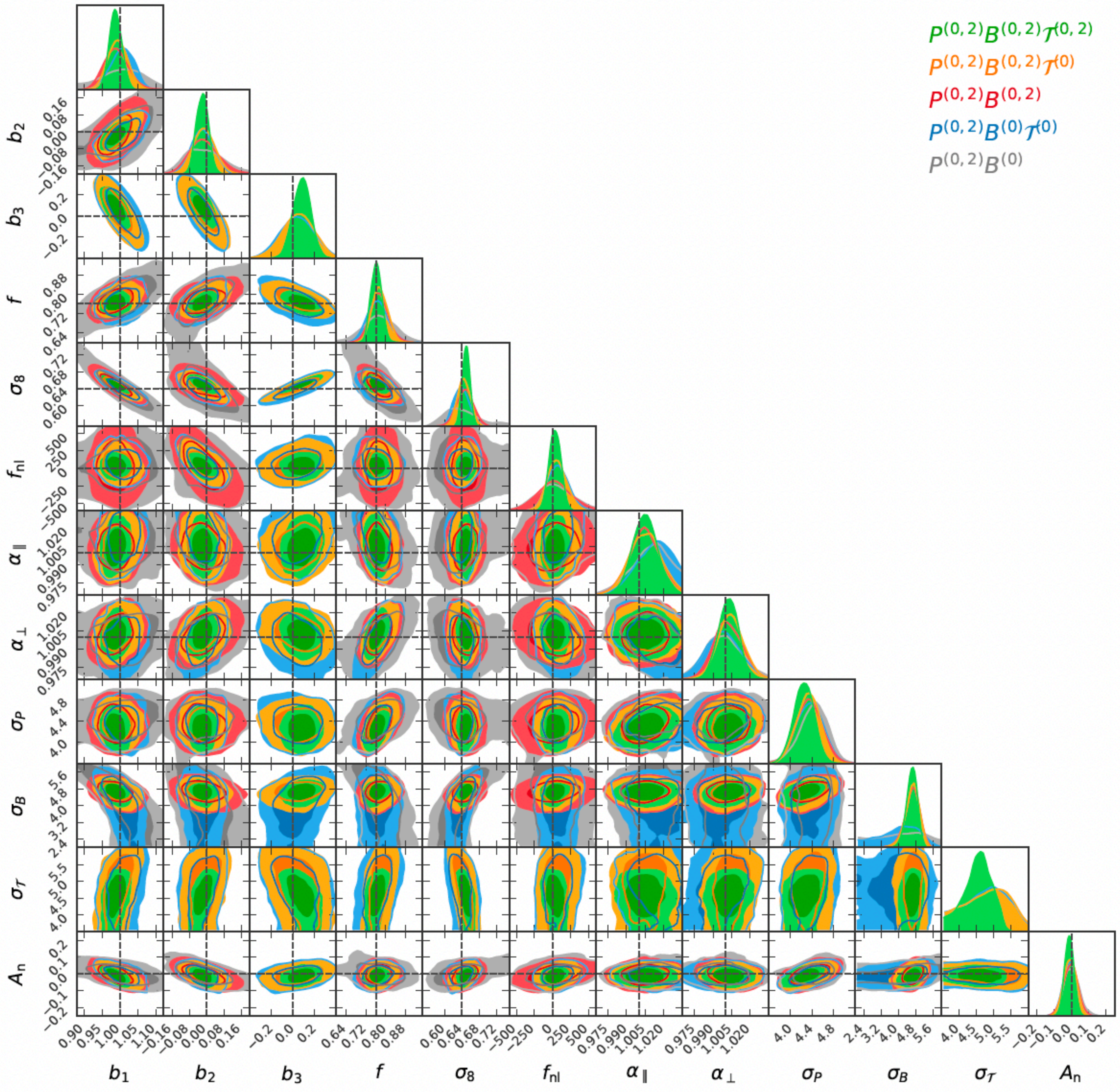

Bonus Slides

Full model data-vector

Power Spectrum

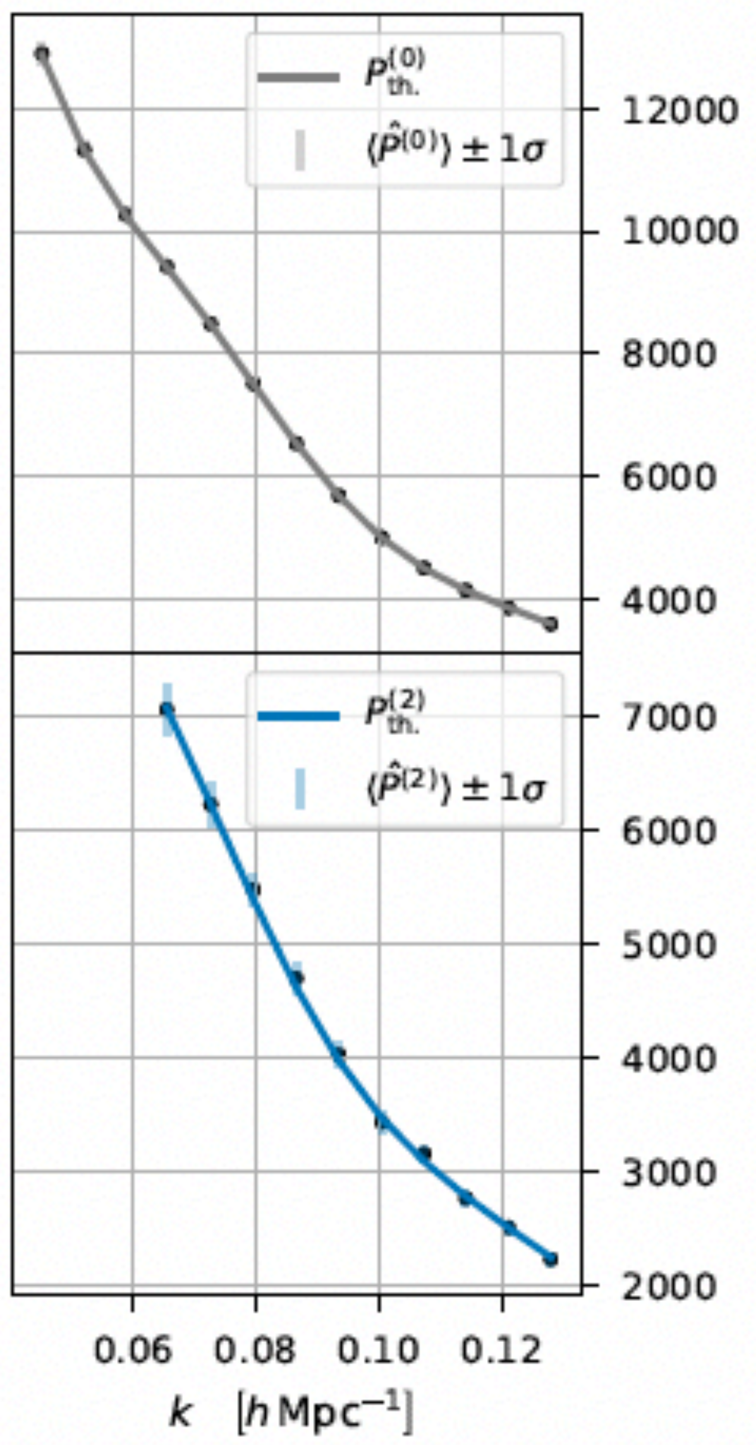

Bispectrum

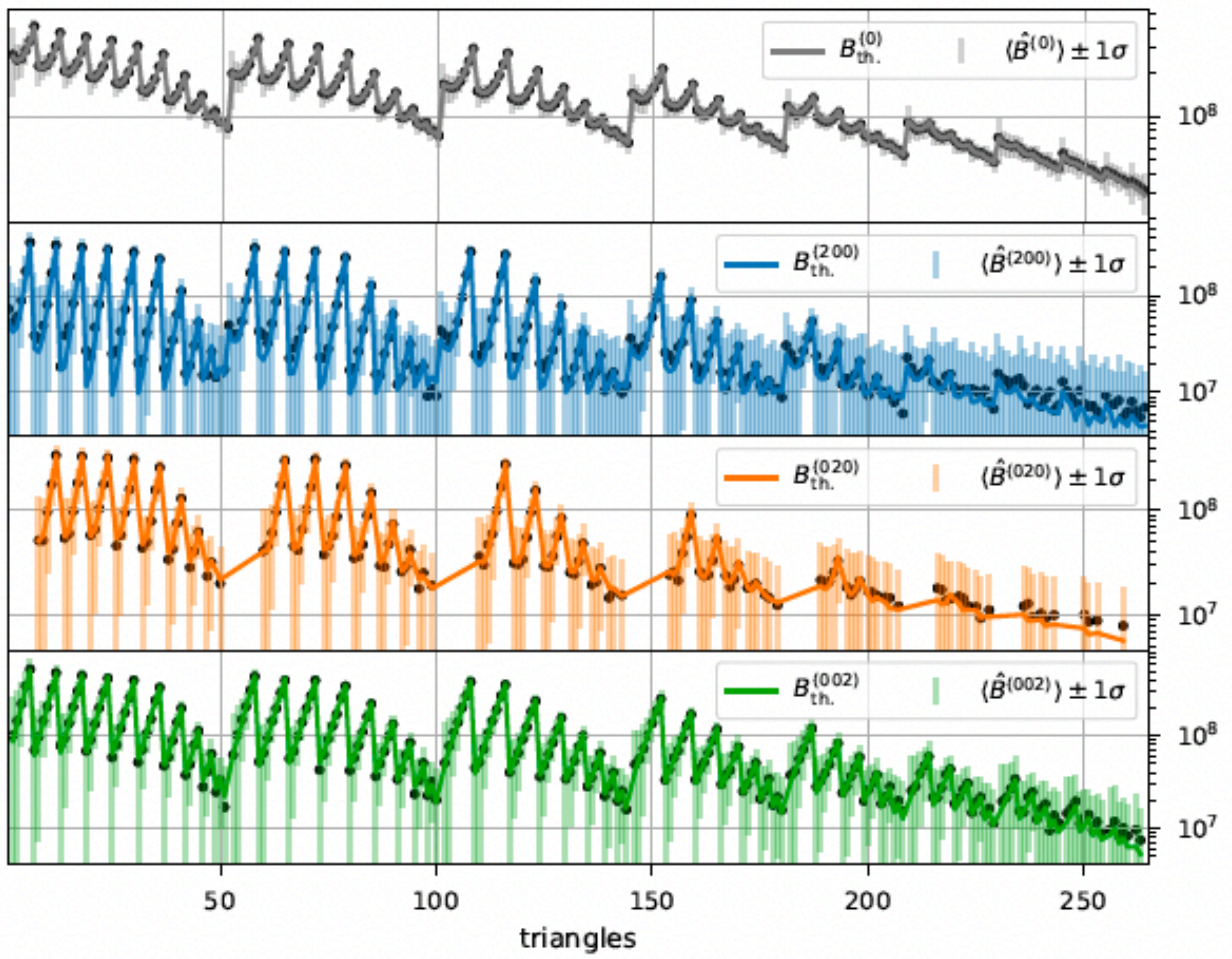

Trispectrum

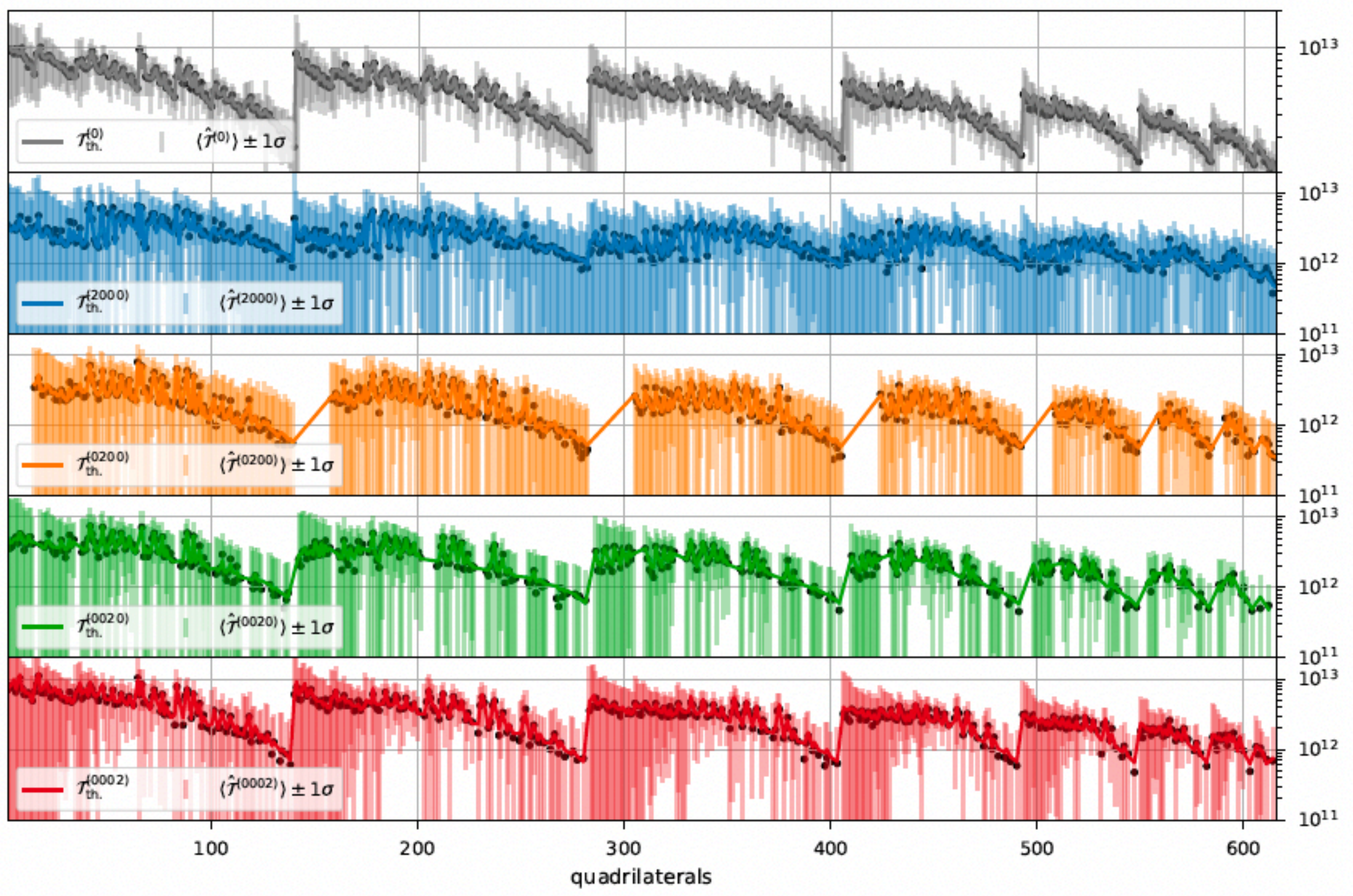

Bonus Slides

Full model data-vector: Ratios

Power Spectrum

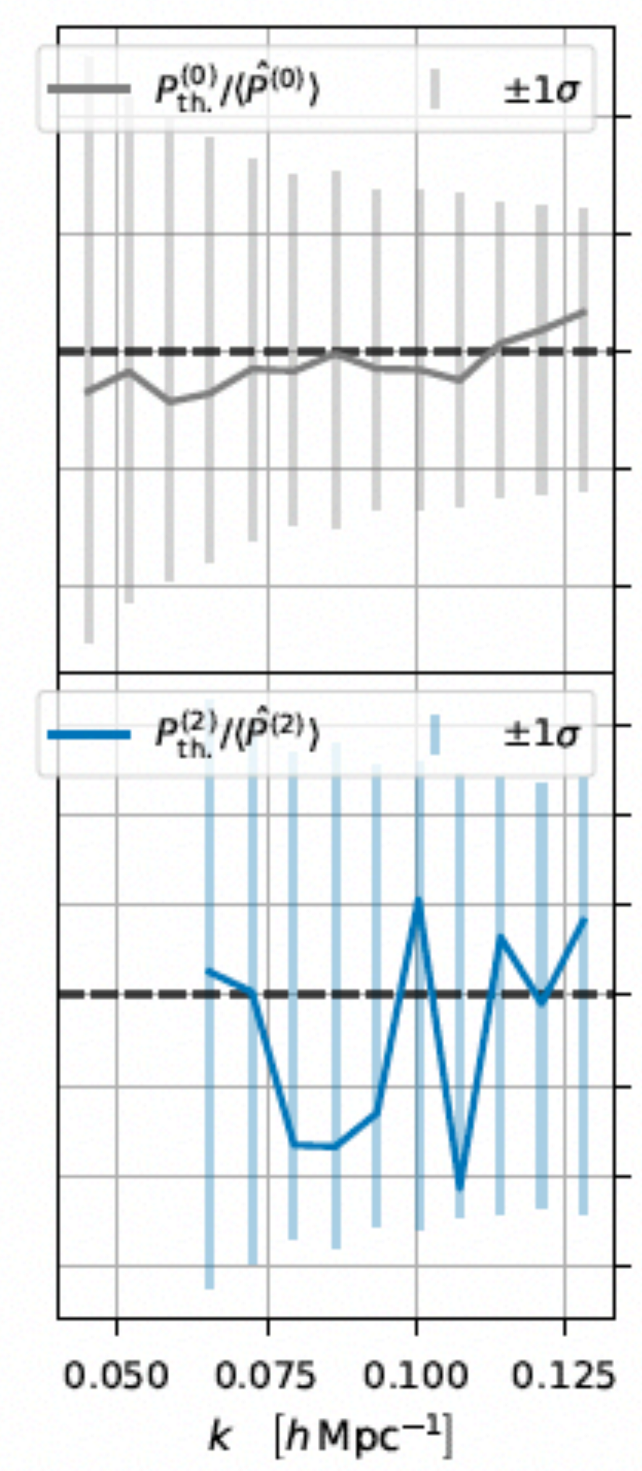

Bispectrum

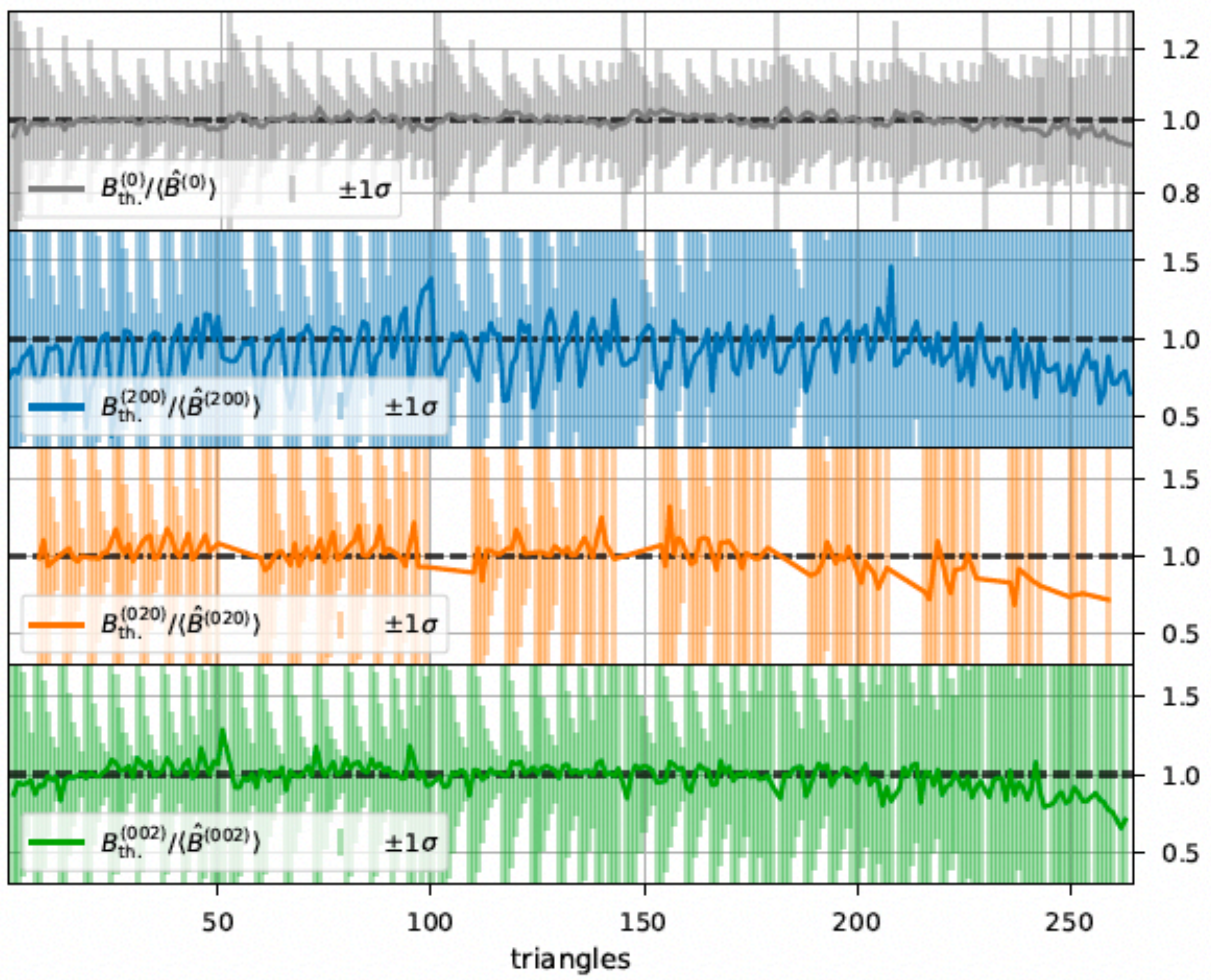

Trispectrum

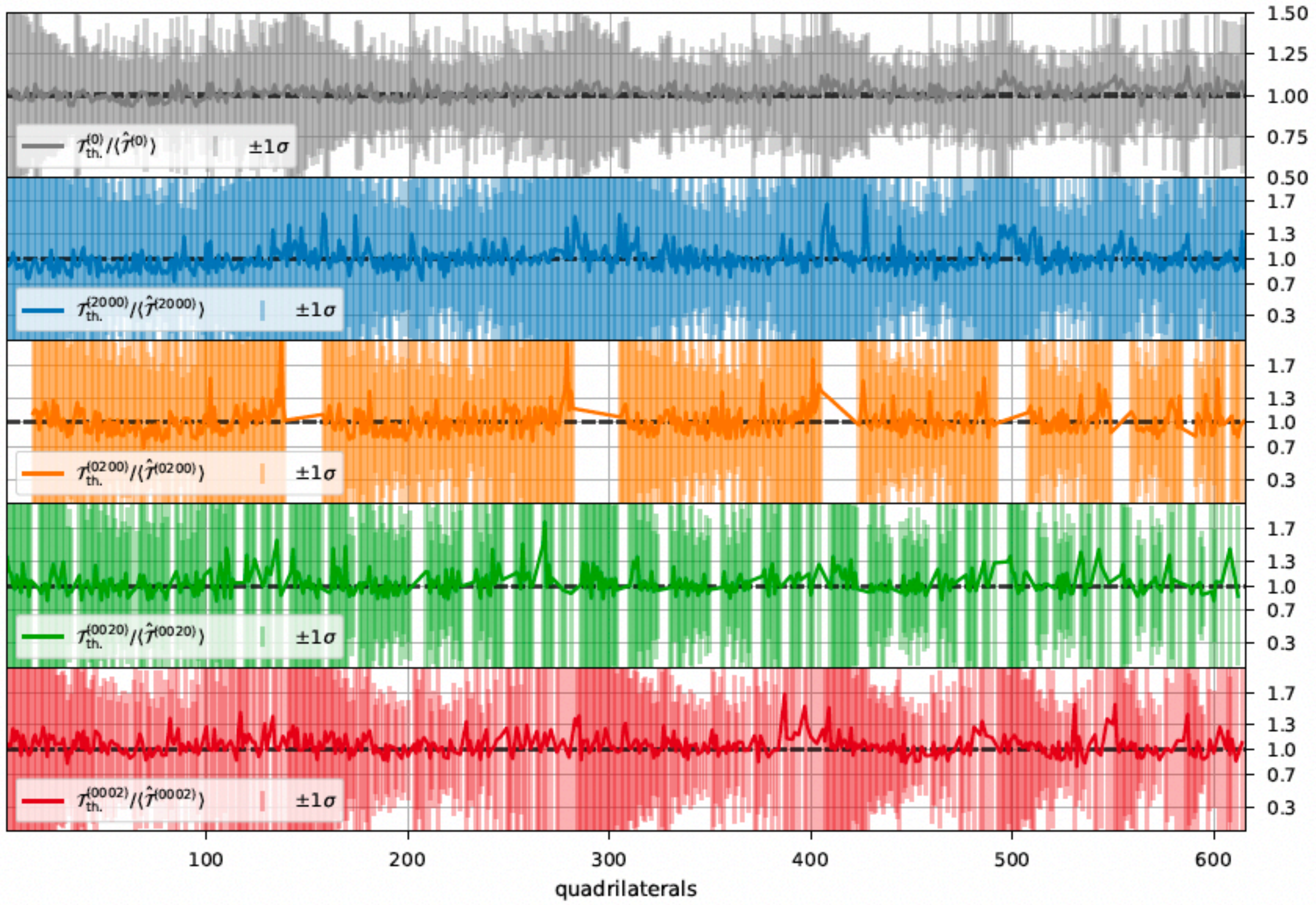

Bonus Slides

f_{nl}=0 results

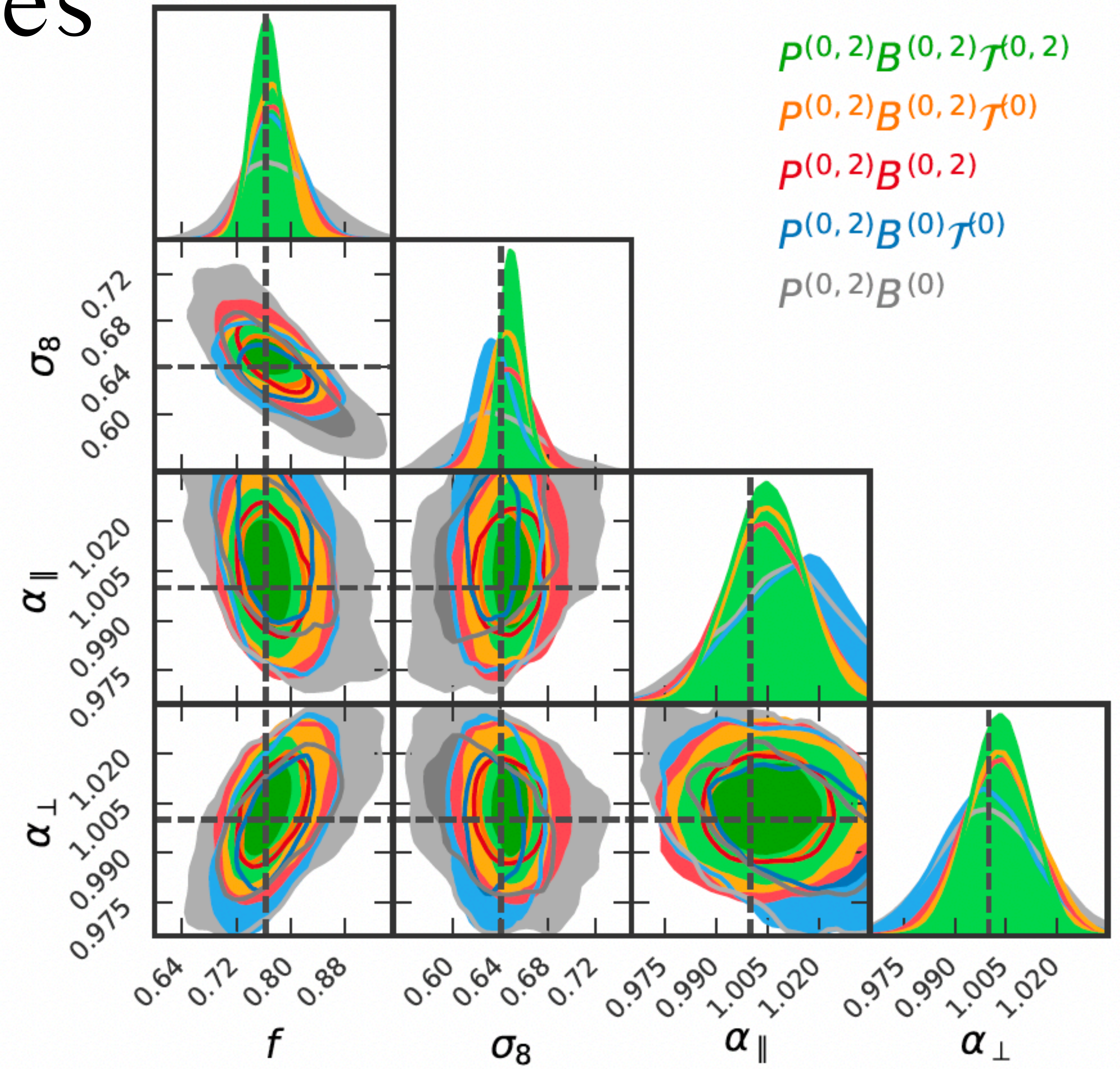

Bonus Slides

FPT model parameters

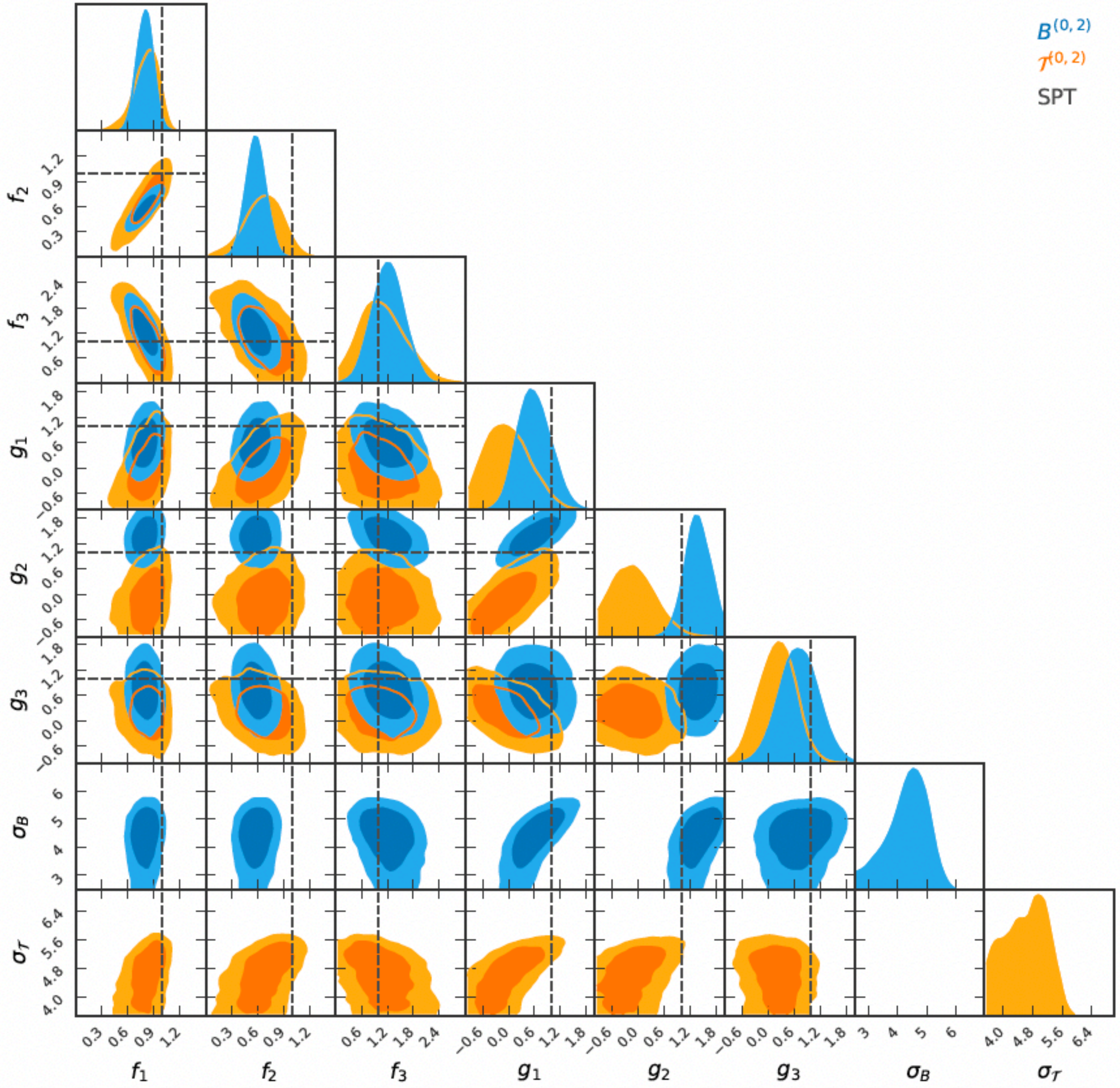

Bonus Slides

Covariance Hartlap Correction precision

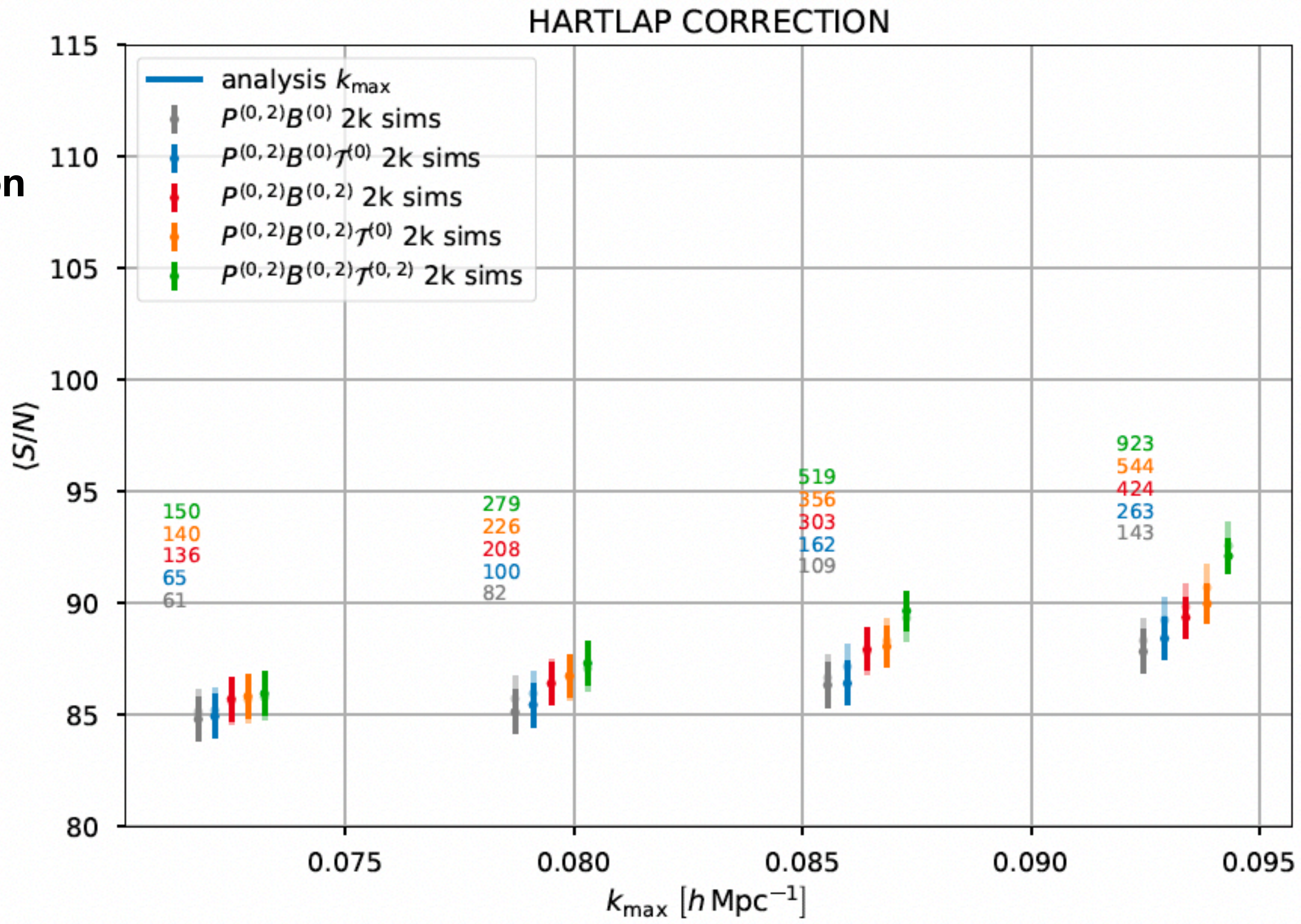

Figure 11. Comparison between the ⟨S/N⟩ computed using 2000 (opaque colours) and 8000 (transparent colours) simulations to estimate the covariance matrices for the different data-vectors combinations, respectively. Applying in both cases the appropriate Hartlap correction the ⟨S/N⟩ remains approximately constant with respect to the number of simulations used.